

Signal Model Consistency Analysis of Different Protocols and Spectral Models in Multi Gradient Echo Liver PDFF and R_2^* Quantification

Mario A. Bacher^{1,2}, Xiaodong Zhong³, Brian M. Dale⁴, Marcel D. Nickel², Berthold Kiefer², Mustafa R. Bashir⁵, Rudolf Stollberger¹, and Stephan A.R. Kannengiesser²
¹Institute of Medical Engineering, Technical University Graz, Graz, Austria, ²MR Applications Development, Siemens AG, Healthcare Sector, Erlangen, Germany, ³MR R&D Collaborations, Siemens Healthcare, Atlanta, GA, United States, ⁴MR R&D Collaborations, Siemens Healthcare, Cary, NC, United States, ⁵Department of Radiology, Duke University Medical Center, Durham, NC, United States

Target Audience: Radiologists, MR physicists.

Purpose: Recently, MR quantification methods for liver fat and iron have gained high interest. In order to make results transferrable and comparable, they should be independent of instrument and minor details of the measurement protocol. It has been shown that this can be achieved for multi-echo gradient echo imaging with simultaneous estimation of proton density fat fraction $PDFF$ and transverse relaxation rate R_2^* ¹⁻³. Many advanced quantification methods use a pre-calibrated fat spectral model; while several have been proposed, e.g.⁴⁻⁶, we know of no systematic comparison.

Previous works on the validation of quantification techniques used comparisons with relaxation corrected multi-echo single voxel spectroscopy for $PDFF$, self-consistency measures, e.g. reconstructions from different subsets of echoes, for R_2^* , and numeric raw data with modelling of confounding effects for both. Here, we use model consistency metrics, and compare different protocol settings and spectral models for in-vivo measurements.

Methods: Twenty healthy volunteers were scanned at 3T (MAGNETOM Skyra, Siemens, Erlangen, Germany). Multi-echo 3D gradient echo (GRE) images of the whole liver were acquired, and processed inline with a multi-step adaptive fitting approach for simultaneous $PDFF$ and R_2^* estimation accounting for confounding effects of relaxation and the multi-peak fat spectrum³.

Base sequence parameters were: 6 echoes, 4° flip angle, FoV ~400mm, 60x4mm slices, breath-hold duration 15-20s. 3 protocol variants were compared according to Table 1. Fat spectral models were varied during the reconstruction by restarting the scanner inline reconstruction of the same original measurement data with modified parameters. The fat spectral model parameters are listed in Table 2.

	TR / ms	TE / ms	matrix	iPAT
a	9.2	1.23, 2.46, 3.7, 4.9, 6.2, 7.4	192	x3
b	16.6	1.23, 2.46, 3.7, 6.2, 9.8, 14.8	128	x4
c	16.6	1.06, 2.20, 3.7, 6.2, 9.8, 14.8	128	x4

Table 1: Protocols. a has consecutive opposed- and in-phase echoes, b is designed for longer, and c additionally for shorter relaxation rates

A ⁴	-3.73 0.083	-3.33 0.627	-3.04 0.072	-2.60 0.096	-2.38 0.066	-1.86 0.015	-	0.68 0.042
B ⁵	-3.80 0.088	-3.40 0.700	-	-2.60 0.120	-	-1.95 0.006	-0.50 0.039	0.60 0.047
C ⁶	-3.83 0.080 * exp(-j·0.45)	-3.47 0.700	-	-2.75 0.084 * exp(j·0.38)	-	-1.87 0.015 * exp(-j·2.80)	-0.50 0.050 * exp(j·0.35)	0.53 0.071 * exp(-j·0.51)

Table 2: Fat spectral models: chemical shift in ppm relative to the water resonance frequency | amplitude (complex: * phasor) for each fat peak

To assess the goodness of fit, relative fitting error maps ς were calculated pixel by pixel from $PDFF$ and R_2^* , the original magnitude images s_n , and the model-predicted images \tilde{s}_n of echo n with echo time TE_n , according to

$$\varsigma = \sqrt{\sum_n (s_n - \tilde{s}_n)^2 / \sum_n s_n^2} \quad \tilde{s}_n = |(W + c_n F) \cdot E_n| \quad c_n = \sum_k a_k \cdot \exp(j2\pi f_0 \cdot v_k \cdot TE_n) \quad E_n = \exp(-R_2^* \cdot TE_n) \quad PDFF = \frac{F}{W + F}$$

where W and F are the reconstructed water and fat images, and c_n are complex factors calculated from the fat spectral model with relative frequencies v_k and amplitudes a_k of the peaks from Table 2. E_n is the relaxation term, and f_0 is the adjusted water resonance frequency. The resulting parameter maps were evaluated in Matlab (MathWorks, Natick, MA, USA): polygonal regions of interest (ROI) were placed interactively in a mid-hepatic slice, avoiding major blood vessels; mean values of the maps of ς , $PDFF$, and R_2^* in the ROI were calculated automatically as data points for further analysis.

Figure 1 shows an example ς map and ROI. Statistical analysis was done in R (R Foundation for Statistical Computing, Vienna, Austria). A p-value of 0.05 was used as threshold for statistical significance.

Results: From the 180 data samples (combinations of volunteer, protocol and fat spectral model), 20 were excluded because of obvious failure of the algorithm like fat/water swaps ($PDFF > 50\%$ or $R_2^* < 10\text{s}^{-1}$). The remaining data samples had values in the following ranges: $1.3\% < \varsigma < 24.5\%$ (mean 4.1%, std 4.1%), $1.5\% < PDFF < 20\%$ (mean 5.5%, std 4.3%), $16.1\text{s}^{-1} < R_2^* < 71.8\text{s}^{-1}$ (mean 44.1s^{-1} , std 9.9s^{-1}).

Figure 2 shows a comparison of the average ROI ς values for different combinations of protocols and fat spectral models.

Friedman tests and post hoc testing revealed that, for each protocol, there were no significant differences in $PDFF$ values, but in R_2^* values. For each spectral model, there were significant differences in $PDFF$ and R_2^* values. For each protocol, there was no significant difference in ς values between spectral models. For each spectral model, there were significant differences in ς values between protocols a-b and a-c, but not between b-c. The lowest average ς values were found for protocol a (Fig. 2).

Conclusion: Model consistency analysis is a useful tool for evaluating multi gradient echo imaging with advanced model based quantification. In this study, the $PDFF$ is largely independent of the acquisition protocol; all spectral models give similar results; the protocol with consecutive opposed- and in-phase echoes resulted in the lowest average fitting errors. The results so far apply to low $PDFF$ and R_2^* values only, but this range may be important to detect abnormal conditions. Future analyses aim at correlating goodness of fit with other accuracy metrics, and for a patient population, including higher $PDFF$ values.

References:

1. Reeder SB *et al.* 2001; JMRI 34:729
2. Hernando D *et al.* 2013; MRM 70:1319
3. Zhong X *et al.* 2013; MRM (in press)
4. Ren J *et al.* 2008; J Lipid Res 49:2055
5. Hamilton G *et al.* 2011; NMR Biomed 24:784
6. Hernando D *et al.* 2010; MRM 64:811

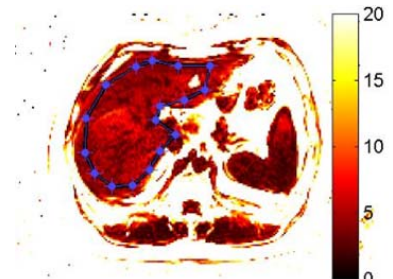


Figure 1: example map of relative fitting error; mean ROI value is 5.2%

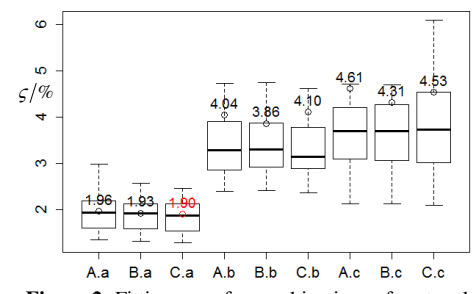


Figure 2: Fitting error for combinations of protocol and fat spectral model. Circles: mean, boxes: median / IQR, whiskers: 95% percentiles